

# Charge instabilities of the two-dimensional Hubbard model with attractive nearest neighbour interaction

**Raymond Frésard**

Laboratoire CRISMAT, UMR 6508 CNRS-ENSICAEN, Caen, France

**Kevin Steffen and Thilo Kopp**

Center for Electronic Correlations and Magnetism, EP VI, Institute of Physics, University of Augsburg, 86135 Augsburg, Germany

E-mail: [Raymond.Fresard@ensicaen.fr](mailto:Raymond.Fresard@ensicaen.fr)

**Abstract.** Attractive non-local interactions jointly with repulsive local interaction in a microscopic modelling of electronic Fermi liquids generate a competition between an enhancement of the static charge susceptibility—ultimately signalling charge instability and phase separation—and its correlation induced suppression. We analyse this scenario through the investigation of the extended Hubbard model on a two-dimensional square lattice, using the spin rotation invariant slave-boson representation of Kotliar and Ruckenstein. The quasiparticle density of states, the renormalised effective mass and the Landau parameter  $F_0^s$  are presented, whereby the positivity of  $F_0^s - 1$  constitutes a criterion for stability. Van Hove singularities in the density of states support possible charge instabilities. A (negative) next-nearest neighbour hopping parameter  $t'$  shifts their positions and produces a tendency towards charge instability even for low filling whereas the  $t'$ -controlled particle-hole asymmetry of the correlation driven effective mass is small. A region of instability on account of the attractive interaction  $V$  is identified, either at half filling in the absence of strong electronic correlations or, in the case of large on-site interaction  $U$ , at densities far from half filling.

## 1. Introduction

Attractive nearest neighbour interactions are commonly introduced in electronic lattice models in order to study (unconventional) superconductivity. However, an attractive non-local interaction can also cause a very different phenomenon in the electronic system; in particular, it can generate charge instabilities. In this paper we focus on the tendency towards charge instabilities in two-dimensional (2D) electronic systems which are simultaneously characterised by electronic correlations. Through their correlations the electrons constitute a Fermi liquid, with non-zero Landau parameters and enhanced effective mass. The Fermi liquid behaviour is expected to break down, especially if the correlations are strong close to half filling or when the attractive nearest neighbour interaction dominates.

It is quite conceivable that the on-site interaction of electrons is repulsive whereas the nearest neighbour interaction becomes attractive. Typically, the on-site Coulomb interaction at transition-metal ions is strongly screened by the polarisation of neighbouring atoms, e.g., oxygen ions in cuprates [1, 2]. Yet the screening depends on the local excitations of a cluster of atoms—for example, on the virtual excitations related to charge transfer in  $\text{CuO}_6$ -octahedra—and can

be different for nearest neighbour Coulomb interaction as compared to the local screening or the Lindhard-type screening for longer distances. Coupling to other degrees of freedom [3], such as a strong electron-lattice coupling, may in combination with screening produce an attractive nearest neighbour interaction, as in certain iron-pnictides [4].

In recent years, metallic two-dimensional electron systems were identified at the interface between two insulating films in oxide heterostructures [5, 6]. In contrast to semiconductor interfaces the electronic states in the oxide materials are confined to few atomic layers in the vicinity of the interface (see, e.g. Ref. [7]). Electronic correlation effects have been observed in scanning tunnelling spectroscopy [8], and the electron system was characterised as a 2D electron liquid. Moreover, the compressibility, which is manifestly related to the Landau Fermi-liquid parameter  $F_0^s$ , was experimentally observed to be negative in a regime of low charge carrier density [9]—the latter being tuned by a backgate bias.

For the Hubbard model [10], Landau parameters were calculated by Vollhardt [11] within Gutzwiller approximation. Recently, Lhoutellier *et al.* [12] calculated the Landau parameters  $F_0^s$  and  $F_0^a$  for an extended three-dimensional Hubbard model within a spin rotation invariant generalisation [13, 14] of the Kotliar and Ruckenstein slave-boson (KRSB) representation [15]. For a 2D system the Hubbard model extended by intersite Coulomb interaction and electron-phonon coupling was shown, within a KRSB evaluation, to produce inhomogeneous polaronic states [16], a scenario which may well be realised in some heterostructures. In the present paper we are concerned with a 2D system and we use the same scheme as in Ref. [12] to evaluate the effective mass  $m^*$  and  $F_0^s$  with focus on attractive non-local interactions and the ensuing charge instabilities. Specifically, we investigate their respective filling dependence. Do electronic correlation effects compete with the tendency towards charge separation?

The KRSB representation was introduced to realise the interaction driven Brinkman-Rice metal-to-insulator transition [17] but since then, it has been successfully used to analyse and characterise antiferromagnetic [18, 19], ferromagnetic [20], spiral [21, 22, 23, 24] and striped [25, 26, 27, 28] phases. KRSB evaluations have been tested against quantum Monte Carlo simulations: A quantitative agreement for charge structure factors was demonstrated [29] and, for example, a very good agreement on the location of the metal-to-insulator transition for the honeycomb lattice has been shown [30]. Also the comparison of ground state energies to numerical solutions [21] or exact diagonalisation data are excellent [23].

The paper is organised as follows: The extended Hubbard model is introduced in Sec. 2, together with its Kotliar and Ruckenstein spin rotation invariant slave-boson representation. In Sec. 3 the saddle-point approximation is presented, jointly with the resulting system of coupled nonlinear equations. Fluctuations are captured within the one-loop approximation, Sec. 4, which allows to determine analytically the Landau parameter  $F_0^s$  at half filling for the pure Hubbard model. Numerical results are discussed in Sec. 5, where we address the filling dependence of  $F_0^s$  and charge instabilities. The paper is summarised in Sec. 6.

## 2. Extended Hubbard model

Anderson's suggestion that the simplest model for the  $d$ -electrons within the  $\text{CuO}_2$  layers common to high- $T_c$  superconductors is the Hubbard model [31] stimulated tremendous research on its properties. However, in the Hubbard model the Coulomb interaction is restricted to the on-site contribution only. In fact, Hubbard himself already argued [10] that for transition metals the matrix elements corresponding to nearest neighbour Coulomb repulsion are relatively large and cannot be disregarded *a priori*. The extended Hubbard model,

$$H = \sum_{i,j,\sigma} t_{ij} c_{i\sigma}^\dagger c_{j\sigma} + U \sum_i \left( n_{i\uparrow} - \frac{1}{2} \right) \left( n_{i\downarrow} - \frac{1}{2} \right) + \frac{1}{2} \sum_{i,j} V_{ij} (1 - n_i)(1 - n_j), \quad (1)$$

takes this notion into account by including intersite Coulomb  $V_{ij}$  interactions. Although these elements decay fast with increasing distance  $|\vec{R}_i - \vec{R}_j|$ , they extend in general beyond nearest neighbours. Here  $c_{i\sigma}^\dagger$  denotes electron creation operators at site  $i$  with spin  $\sigma$ , and  $n_{i\sigma} = c_{i\sigma}^\dagger c_{i\sigma}$ . The particle-hole symmetric form for both density-density interaction terms is used throughout this work.

In our numerical evaluations below, we restrict the matrix elements  $t_{ij}$  to  $-t$  for  $(i, j)$  a pair of nearest neighbour sites and to  $-t'$  for next-nearest neighbour pairs on a square lattice. All other  $t_{ij}$  are set to zero. While the bare intersite Coulomb interactions are repulsive, the effective parameters  $\{V_{ij}\}$  may become attractive if the coupling to other subsystems is considered [3]. An example is strong electron-lattice coupling, which induces a local lattice deformation surrounding the electron. Under certain conditions such electronic polarons may attract each other as, for example, in some iron-pnictides [4]. Since we are interested in instabilities indicated by  $F_0^s \leq -1$ , we limit our numerical calculations in this paper to  $V_{ij} \leq 0$ .

In the spin rotation invariant (SRI) Kotliar and Ruckenstein slave-boson (KRSB) representation [13, 14], which we adopt for our study, one introduces the auxiliary canonical fermionic  $f_\sigma$ , and bosonic  $e$ ,  $p_0$ ,  $\vec{p}$ , and  $d$  particles to represent the physical states as:

$$\begin{aligned} |0\rangle &= e^\dagger |\text{vac}\rangle \\ |\sigma\rangle &= \sum_{\sigma'} p_{\sigma\sigma'}^\dagger f_{\sigma'}^\dagger |\text{vac}\rangle \quad \sigma = \uparrow, \downarrow \\ |2\rangle &= d^\dagger f_{\uparrow}^\dagger f_{\downarrow}^\dagger |\text{vac}\rangle, \end{aligned} \quad (2)$$

with  $\underline{p}^\dagger = \frac{1}{2} \sum_{\mu=0}^3 p_\mu^\dagger \underline{\tau}^\mu$ , and  $\underline{\tau}^\mu$  the Pauli matrices. In terms of these auxiliary operators the Hamiltonian Eq. (1) reads

$$\begin{aligned} H &= \sum_{i,j} t_{ij} \sum_{\sigma\sigma'\sigma_1} z_{i\sigma_1\sigma}^\dagger f_{i\sigma}^\dagger f_{j\sigma'} f_{j\sigma'\sigma_1} + U \sum_i \left( d_i^\dagger d_i - \frac{1}{2} \sum_\sigma f_{i\sigma}^\dagger f_{i\sigma} + \frac{1}{4} \right) \\ &+ \frac{1}{4} \sum_{i,j} V_{ij} \left[ \left( 1 - \sum_\sigma f_{i\sigma}^\dagger f_{i\sigma} \right) Y_j + Y_i \left( 1 - \sum_\sigma f_{j\sigma}^\dagger f_{j\sigma} \right) \right]. \end{aligned} \quad (3)$$

The spin and charge degrees of freedom are mapped onto bosons in this representation; further details are given in Refs. [32] and [12]. We now suppress the site indices in expressions where their reintroduction is self-evident. Above, we introduced the hole doping operator

$$Y \equiv e^\dagger e - d^\dagger d, \quad (4)$$

while  $\underline{z}$  is given by:

$$\underline{z} \equiv e^\dagger \underline{L} \underline{M} \underline{R} \underline{p} + \tilde{p}^\dagger \underline{L} \underline{M} \underline{R} d \quad (5)$$

where  $\tilde{p}_{\sigma\sigma'} = (\delta_{\sigma,\sigma'} - \delta_{\sigma,-\sigma'}) p_{-\sigma',-\sigma}$  and

$$\begin{aligned} \underline{M} &= \left[ 1 + e^\dagger e + \sum_\mu p_\mu^\dagger p_\mu + d^\dagger d \right]^{\frac{1}{2}}, \\ \underline{L} &= \left[ \left( 1 - d^\dagger d \right) \underline{1} - 2 \underline{p}^\dagger \underline{p} \right]^{-\frac{1}{2}}, \\ \underline{R} &= \left[ \left( 1 - e^\dagger e \right) \underline{1} - 2 \tilde{p}^\dagger \tilde{p} \right]^{-\frac{1}{2}}. \end{aligned} \quad (6)$$

The tensor  $\underline{z}$  may also be expanded in terms of Pauli matrices as  $\underline{z} = \sum_{\mu=0}^3 z_{\mu} \underline{T}^{\mu}$ . The new Fock space depends in this representation on eight auxiliary operators. The resulting unphysical degrees of freedom may be eliminated through five local constraints,

$$e^{\dagger}e + \sum_{\mu} p_{\mu}^{\dagger}p_{\mu} + d^{\dagger}d = 1, \quad (7)$$

$$\sum_{\sigma} f_{\sigma}^{\dagger}f_{\sigma} = \sum_{\mu} p_{\mu}^{\dagger}p_{\mu} + 2d^{\dagger}d, \quad (8)$$

$$\sum_{\sigma,\sigma'} f_{\sigma'}^{\dagger}\vec{\tau}_{\sigma\sigma'}f_{\sigma} = p_0^{\dagger}\vec{p} + \vec{p}^{\dagger}p_0 - i\vec{p}^{\dagger} \times \vec{p}, \quad (9)$$

which are enforced within the path integral formalism and have to be satisfied for each lattice site.

In the SRI KRSB representation the phases of the  $e$  and  $p_{\mu}$  bosons are gauged away by promoting all constraint parameters to fields [14], and they remain as radial slave-boson fields [33]. Their exact expectation values are generically non-vanishing even though bose condensation is excluded by local gauge invariance [34]. In contrast, the slave-boson field corresponding to double occupancy  $d$  is still complex [14, 35, 36].

The saddle-point approximation introduced in the next section is exact in the large degeneracy limit, with Gaussian fluctuations generating the  $1/N$  corrections [14], and obeys a variational principle in the limit of large spatial dimensions. In this limit the Gutzwiller approximation becomes exact for the Gutzwiller wave function and longer ranged interactions are static and reduce to their Hartree approximation [37, 38]. On these grounds, the approximation used here to the extended Hubbard model Eq. (1) complies with a variational principle in the limit of large spatial dimensions.

Due to the formal properties mentioned above, our approach covers properties of strongly correlated electrons, as, e.g., the suppression of the quasiparticle residue and the formation of a charge gap at the Mott-Hubbard transition, and the Brinkman-Rice transition [17] to an insulating state at half filling with increasing on-site Coulomb interaction. The impact of the non-local interaction on the latter transition is of particular interest.

### 3. Saddle-point approximation

Ideally the functional integrals should be calculated exactly. Regarding spin models this has been achieved for the Ising chain [33], but in the case of interacting electron models exact evaluations could be performed on small clusters only, either using the Barnes representation [34], or the Kotliar and Ruckenstein representation [39]. Such a calculation remains challenging on lattices of higher dimensionality, and we here rather resort to the saddle-point approximation. The presentation here for the 2D electronic system follows closely that of Ref. [12] where a 3D extended Hubbard model was investigated. In the translational invariant paramagnetic phase all the local quantities are site independent, and the action at saddle-point reads ( $\beta = 1/k_B T$ ),

$$S = \beta L \left( S_B + S_F + \frac{1}{4}U \right), \quad (10)$$

where  $L$  is the number of lattice sites and

$$S_B = \alpha(e^2 + d^2 + p_0^2 - 1) - \beta_0(p_0^2 + 2d^2) + U d^2 + \frac{1}{2}V_0 Y, \quad (11)$$

$$S_F = -\frac{1}{\beta} \sum_{\vec{k},\sigma} \ln \left( 1 + e^{-\beta E_{\vec{k}\sigma}} \right). \quad (12)$$

Here  $\alpha$  and  $\beta_0$  are site-independent Lagrange multipliers that enforce the constraints Eq. (7) and Eq. (8), respectively. For the extended Hubbard model (1) the quasiparticle dispersion in Eq. (12) reads:

$$E_{\vec{k}\sigma} = z_0^2 t_{\vec{k}} + \beta_0 - \frac{1}{2}U - \frac{1}{2}V_0 Y - \mu, \quad (13)$$

Here  $z_0^2$  represents the inverse effective mass  $m/m^*$  correction, exclusively caused by correlation effects. The Fourier transform of the intersite Coulomb repulsion is

$$V_{\vec{k}} = \frac{1}{L} \sum_{i,j} V_{ij} e^{-i\vec{k} \cdot (\vec{R}_j - \vec{R}_i)}. \quad (14)$$

It is worth mentioning that only  $V_{\vec{k}=0}$  enters Eq. (13). The saddle-point equations following from Eq. (10) read:

$$\begin{aligned} p_0^2 + e^2 + d^2 - 1 &= 0, \\ p_0^2 + 2d^2 &= n, \\ \frac{1}{2e} \frac{\partial z_0^2}{\partial e} \bar{\varepsilon} + \frac{1}{2} V_0 (1-n) \frac{1}{2e} \frac{\partial Y}{\partial e} &= -\alpha, \\ \frac{1}{2p_0} \frac{\partial z_0^2}{\partial p_0} \bar{\varepsilon} &= \beta_0 - \alpha, \\ \frac{1}{2d} \frac{\partial z_0^2}{\partial d} \bar{\varepsilon} + \frac{1}{2} V_0 (1-n) \frac{1}{2d} \frac{\partial Y}{\partial d} &= 2\beta_0 - \alpha - U. \end{aligned} \quad (15)$$

Here we have introduced the averaged kinetic energy,

$$\bar{\varepsilon} = \int d\epsilon \rho(\epsilon) \epsilon f_F(z_0^2 \epsilon + \beta_0 - \frac{1}{2}U - \frac{1}{2}V_0 Y - \mu), \quad (16)$$

the determination of which involves the density of states  $\rho(\epsilon)$  and  $f_F(\dots)$  is the Fermi function. The density of states (DOS) is displayed in Fig. 1(a) for various values of  $t'$ . With  $y \equiv (e+d)^2$  and the doping away from half filling  $\delta = 1 - n$ , the equations Eqs. (15) may be merged into a single one:

$$y^3 + (u-1)y^2 = u\delta^2, \quad (17)$$

where the Coulomb parameter is conveniently expressed in units of  $U_0$  as  $u = U/U_0$  with

$$U_0 = -\frac{8}{1-\delta^2} \bar{\varepsilon}. \quad (18)$$

The three solutions of Eq. (17) have been discussed in much detail at zero temperature in Ref. [14], with the result that they entail one single critical point located at the Brinkman-Rice transition [17]. It signals a second order transition. At finite temperature, a line of first order transitions with coexistence of phases is found [30]. On the contrary, a finite Hund's coupling in a two-band model induces coexistence of one good and one poor metallic phase at and in the vicinity of half filling at zero temperature [40].

Returning to the one-band model at  $\delta = 0$ , the inverse effective mass  $m/m^* = z_0^2$  may be obtained as

$$z_0^2 = 1 - u^2. \quad (19)$$

Therefore a metal-to-insulator transition occurs at half filling for a given lattice at  $U_c$ , which is defined as follows

$$U_c \equiv \lim_{\delta \rightarrow 0} U_0 = -8\bar{\varepsilon}. \quad (20)$$

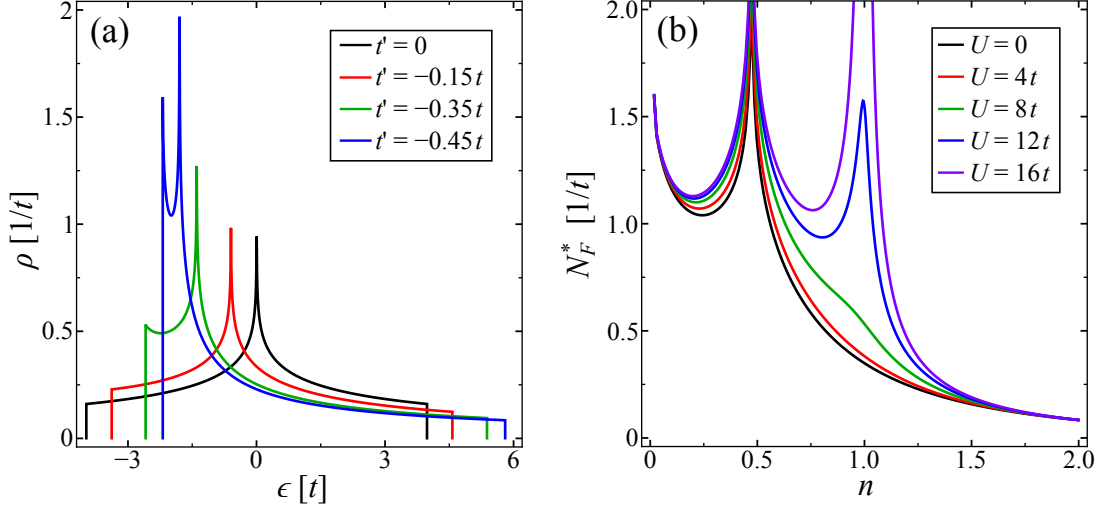


**Figure 1.** Density of states (DOS). *a*) DOS  $\rho(\epsilon)$  of the square lattice for various values of  $t'$  as a function of band energy  $\epsilon$ . *b*) Effective DOS at the Fermi edge  $N_F^*$  for  $t' = -0.45t$  and varying on-site Coulomb interactions  $U$  as a function of filling  $n$ . The effective DOS is independent of the nearest neighbour interaction  $V$ .

A remarkable property of the paramagnetic phase we consider is that  $V_{ij}$  elements do not enter explicitly Eq. (17). Hence, in this paramagnetic phase, the intersite interactions only influence the fluctuations and do not change electron localisation due to strong on-site interaction  $U$ . In particular, neither a nearest neighbour Coulomb interaction  $V_{<i,j>}$  nor a long-ranged one  $V(i-j)$  has influence on the Mott gap as discussed by Lavagna [41]. Furthermore, the double occupancy is in exact agreement with the Gutzwiller approximation as derived by Vollhardt, Wölfle and Anderson [42]. In the present case of a 2D square lattice the double occupancy vanishes at half filling for  $U_c = 12.96t$  with  $t' = 0$ ,  $U_c = 13.06t$  with  $t' = -0.15t$ ,  $U_c = 13.4t$  with  $t' = -0.35t$ , and for  $U_c = 13.62t$  with  $t' = -0.45t$ . Thus, the location of the Brinkman-Rice transition [17] shows little dependence on  $t'$ . Somewhat surprisingly, the effect of the  $t'$ -induced gradual depression of the DOS at half filling and, consequently, the depression of  $U_c$  is opposite to the one found for the semi-metallic honeycomb lattice, for which  $U_c = 12.6t$  was obtained [30].

We here emphasise that Eq. (17) is not only insensitive to  $V_{ij}$  elements, but also to the representation of the Hubbard interaction. Indeed, while it is commonly directly expressed in terms of double occupancy, the presently used particle-hole symmetric form results in the same equation. Hence, the energy depends on the precise form of the interactions but the slave-boson saddle-point values do not.

#### 4. One-loop approximation to the charge response function

The mapping of all degrees of freedom onto bosons allows for directly evaluating the charge response function. According to, e. g., Ref. [12], the density fluctuations may be expressed as

$$\delta N \equiv \sum_{\sigma} \delta n_{\sigma} = \delta(d^{\dagger}d - e^{\dagger}e). \quad (21)$$

With this at hand, the charge autocorrelation functions can be written in terms of the slave-boson correlation functions as:

$$\chi_c(k) = \sum_{\sigma\sigma'} \langle \delta n_{\sigma}(-k) \delta n_{\sigma'}(k) \rangle = \langle \delta N(-k) \delta N(k) \rangle. \quad (22)$$

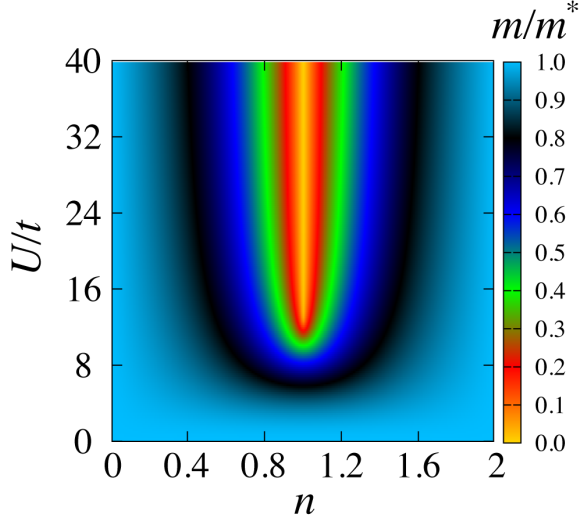


**Figure 2.** Inverse mass renormalisation for the square lattice with  $t' = 0$  as a function of  $n$  and  $U$ . The effective mass  $m^*$  is independent of the nearest neighbour interaction  $V$ .

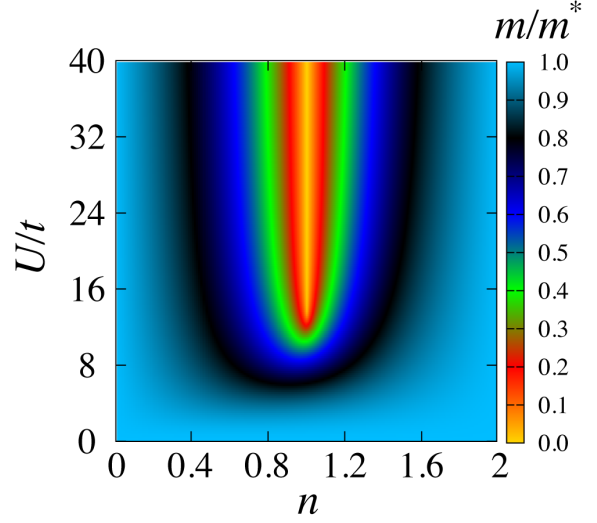


**Figure 3.** Inverse mass renormalisation for the square lattice with  $t' = -0.45t$ . The effective mass  $m^*$  is independent of the nearest neighbour interaction  $V$ .

In the following calculation to one-loop order we use the notation  $k \equiv (\vec{k}, \omega)$ , and the propagator  $S_{ij}(k)$  as given in Ref. [12]. The charge susceptibility results as follows:

$$\chi_c(k) = 2e^2 S_{11}^{-1}(k) - 4ed S_{12}^{-1}(k) + 2d^2 S_{22}^{-1}(k). \quad (23)$$

In the long wavelength and low frequency limit, this relation yields the Landau parameter  $F_0^s$ . In contrast to the conventional random phase approximation (RPA) results, the obtained Landau parameter cannot be brought to a simple analytical form, unless the intersite Coulomb elements  $V_{ij}$  are neglected. In this case, simplifications are most effective at half filling [11, 43, 44], where  $F_0^s$  is determined by:

$$F_0^s = -1 + \frac{1}{(1 - U/U_c)^2}. \quad (24)$$

The impact of the Hubbard  $U$  on  $F_0^s$  is transparent:  $F_0^s$  steadily increases from 0 at  $U = 0$  until it diverges at the metal-to-insulator transition. It should be noted that  $F_0^s$  from Eq. (23) is not sensitive to the details of the intersite elements  $V_{ij}$ , but only to its zero-momentum Fourier transform (Eq. (14)). For concreteness we restrict ourselves below to nearest neighbour interaction — in which case  $V_0 = 4V$  — but our results apply as well to more general situations, provided  $V$  is properly interpreted as  $V = \frac{1}{4} \frac{1}{L} \sum_{i,j} V_{ij}$ .

## 5. Results

In this work, we evaluated the density response from the one-loop result within slave-boson theory and extracted the dimensionless Landau parameter  $F_0^s$  in order to characterise the tendency towards a charge instability through a single effective interaction parameter. Our analysis builds on a 2D lattice model with two interaction scales: A positive on-site Coulomb interaction  $U$ , which may be tuned to target the regime of strong electronic correlations, and a negative nearest neighbour interaction  $V$ , which can drive a charge instability in the case of  $F_0^s \leq -1$ .

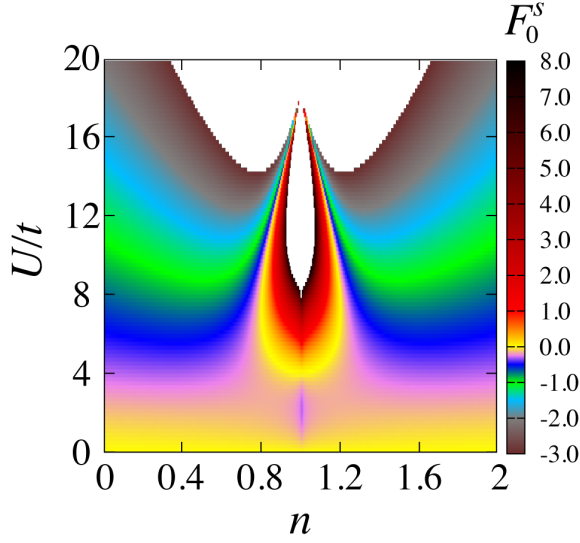


**Figure 4.** Landau parameter  $F_0^s$  for the square lattice as function of  $n$  and  $U$ . Here  $t' = 0$  and  $V/U = -0.2$ .

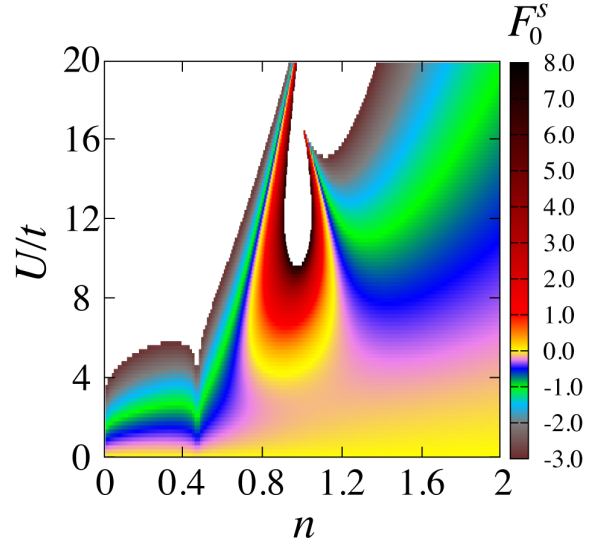


**Figure 5.** Landau parameter  $F_0^s$  for the square lattice. Here  $t' = -0.45t$  and  $V/U = -0.2$ .

The question arises if both characteristics appear in this model simultaneously, namely strong correlations and a charge instability—or are they found in separate regimes that are controlled by the electronic density  $n$ ? Here we may choose to identify strong correlations through a large effective mass  $m^*$ . In fact,  $m/m^*$  is zero at half filling and small in the respective density regime close to half filling (see Figs. 2 and 3). Moreover,  $m/m^*$  is independent of  $V$ . Consistent with Fermi liquid theory, the effective density of states at the Fermi energy  $N_F^*$  is enhanced with  $m^*/m$ , so that one observes three significant structures in  $N_F^*(n)$  for finite  $t'$  and  $U/t \gtrsim 4$  (see Fig. 1(b)): The two lower peaks for  $n \rightarrow 0$  and  $n \simeq 0.5$  represent the Van Hove singularities of the two-dimensional DOS for negative  $t'$  (cf. Fig. 1), whereas the buildup of the peak at  $n = 1$  is a pure correlation effect. For  $t' = 0$  the Van Hove peak and the correlation peak are both placed at  $n = 1$ , whereas a finite  $t'$  serves to keep these peaks apart (which will be helpful also in the discussion of the structure of  $F_0^s$  below).

A graphical survey of the impact of positive  $U$  and negative  $V$  on  $F_0^s(n)$  is provided by Figs. 4 and 5. We keep the ratio  $V/U = -0.2$  constant in these contour plots in order to reduce the number of control parameters. As required,  $F_0^s$  is zero along the  $U = 0 = V$   $n$ -axis. For small values of  $U/t$  (and correspondingly of  $-V/t$ ), the Landau parameter  $F_0^s$  is negative but still larger than  $-1$ , irrespective of filling. Then, at intermediate values of  $U/t$ , the Landau parameter becomes positive close to half filling, whereas it approaches  $-1$  for filling well below or above half filling. The latter behaviour is induced by the negative nearest neighbour interaction  $V$ , whereas the positive value of  $F_0^s$  close to half filling is a correlation effect controlled by the repulsive  $U$ . Eventually, at large  $U/t$  and  $-V/t$ , Fermi liquid behaviour breaks down, connected either with  $m/m^* = 0$  at half filling or with  $F_0^s \leq -1$  for finite doping away from half filling.

For  $t' < 0$  the (particle-hole) symmetry with respect to  $n = 1$  is broken and the charge instability at  $F_0^s < -1$  is attained already for lower values of the interaction parameters for  $n < 1$  (see Fig. 5). This enhancement of the instability applies especially for values of  $n$  at and below the density for which the Van Hove singularity (VHs) produces a peak in the bare  $N_F(n)$ : A dip structure is formed slightly below  $n = 0.5$  (Fig. 5). The VHs is also reflected in the finer dip structure in Fig. 4 at  $n = 1$ , however there, the correlation-induced increase of  $F_0^s$



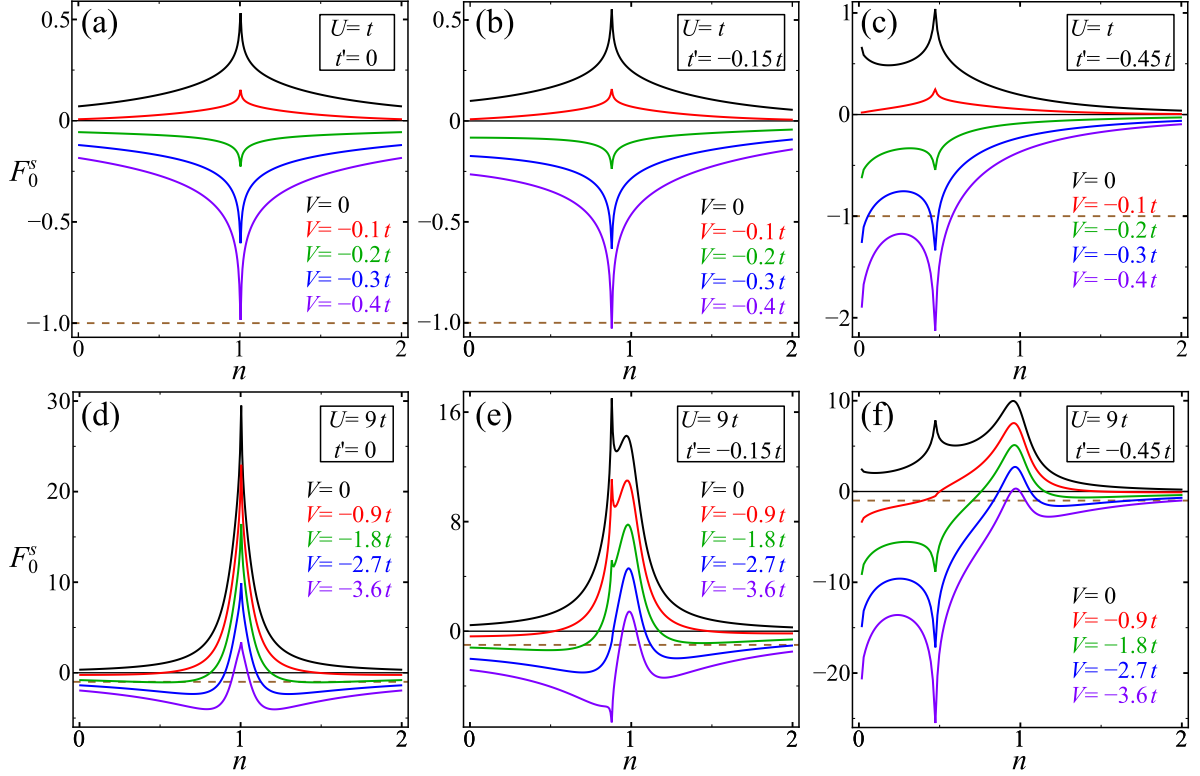


**Figure 6.** Landau parameter  $F_0^s$  for different sets of  $t'$  and  $U$  as function of filling  $n$ . The system becomes unstable for  $F_0^s < -1$ , i.e., below the (brown) dashed line.

and the VHs-controlled decrease of  $F_0^s$  through negative  $V$  compete close to half filling. This will become evident below, when we fix  $U$  and control  $F_0^s$  by  $V$ .

In Fig. 6 we fix  $U/t$  to 1 and 9 in the upper and in the lower set of panels, respectively. In panels (a) and (d) the next-nearest neighbour hopping  $t'$  is zero. For  $V/t = 0$  and  $V/t = -0.1$ ,  $F_0^s$  is positive for all values of  $n$ . For sufficiently negative values of  $V$  ( $V/t \lesssim -0.15$  for  $U/t = 1$  in (a)),  $F_0^s$  is negative for the full range of  $n$ -values. However, for  $V/t \gtrsim -0.4$  the electronic system is still stable against charge fluctuations, as  $F_0^s > -1$  still applies. For  $U/t = 9$  (panel (d)) we observe a peak around  $n = 1$  with  $F_0^s > 0$ . In contrast,  $F_0^s$  is negative for  $n$  not close to half filling, except for  $V = 0$  when  $F_0^s \geq 0$  is always true. Obviously, close to half filling Mott-Hubbard-type electronic correlations compete with the charge instability induced through negative  $V$ . It depends on the ratio of  $U/|V|$  which of them prevails.

For  $t' \neq 0$ , the picture is more clear-cut (Fig. 6, panel (b) and (e)): For weak coupling, that is  $U/t = 1$ , the  $n$ -dependent structure of  $F_0^s$  (peak or dip) is controlled by the position of the VHs (similar to panel (a)). However, for strong coupling  $U/t = 9$ , a smooth peak emerges around  $n = 1$ . This peak was concealed in (d) by the contribution from the VHs (at zero or small  $t'$ ) but becomes visible when the VHs-related peak is shifted to lower values of  $n$  for more negative values of  $t'$ . The shape of the function  $F_0^s$  in dependence on  $n$  is the central result of our work. At half filling the Mott-Hubbard-type correlations dominate assuming that the negative value of  $V$  is not unreasonably large with respect to  $U$ .

Below half filling (for negative  $t'$ ), the position of the VHs determines the peak or dip in  $F_0^s(n)$ —see also panels (c) and (f). It is not unexpected that  $F_0^s(n)$  displays a peak/dip structure controlled by the VHs of the density of states: The dimensionless Landau parameters are composed of a microscopic interaction times the density of states at the Fermi energy.

With this survey of  $F_0^s(n)$  in the  $U$ - $V$  coupling parameter space, the conclusion can be drawn that charge instabilities induced by an attractive  $V$  can only be generated in a regime where strong electronic correlations are absent. The charge instability is boosted by VHS whereas the strong correlations effects are not controlled by VHS.

## 6. Summary

In order to gain a more thorough understanding of correlated two-dimensional electron systems we applied slave-boson theory to an extended Hubbard model. In the Kotliar and Ruckenstein (spin rotation invariant) slave-boson representation it is feasible to interpolate between the non-interacting limit and the strong coupling case. Here we used this slave-boson representation to determine the two prominent parameters of Landau theory,  $m^*/m$  and  $F_0^s$ . Beyond the one-band repulsive Hubbard model, we included a nearest neighbour coupling  $V$  which is, in our investigation, attractive as we wanted to study instabilities in the (static) charge response. The charge response and, correspondingly,  $F_0^s$  were identified in one-loop approximation. While we focused on the effect of nearest neighbour attractive interactions, it should be emphasised that our results for  $F_0^s$  also directly apply to more general situations, as the non-local interaction only enters through its zero-momentum Fourier component. Furthermore, we introduced a next-nearest neighbour hopping  $t'$  in order to control the position of the Van Hove singularity (VHS)—in particular, to shift the VHS from its position in the middle of the band (at  $t' = 0$ ) to lower energies (for  $t' < 0$ ). Thereby we separated the correlation induced enhancement of  $F_0^s$  at half filling from DOS controlled effects.

We found a strong enhancement of  $m^*/m$  close to half filling for  $U/t \gtrsim 10$ , and that mass renormalisation diverges at half filling—in agreement with the standard approaches to the Hubbard model with strong on-site repulsion  $U$ . The effective mass  $m^*$  turns out to be independent of the nearest neighbour interaction  $V$ , at least on the paramagnetic saddle-point level of approximation. Moreover,  $m^*/m$  depends only weakly on  $t'$ . As expected, the effective mass strongly renormalises the DOS at the Fermi edge ( $N_F^*$ ) for half filling and intermediate to large values of  $U/t$ . When the VHS is shifted towards lower energies for  $t' < 0$ , then the peak in  $N_F^*$  centred at half filling is a signature of the correlation-induced mass enhancement, exclusively.

The Landau parameter  $F_0^s$  is zero in the interactionless case. At any finite  $U$  and/or  $V$ , it is zero only for particular values of filling  $n$ , in the case that repulsive  $U$  and attractive  $V$  compete. Higher Landau parameters may then account for the residual interaction between quasiparticles but this has not yet been investigated.

For weak repulsive on-site interaction  $U \simeq t$ , the density dependence of  $F_0^s$  is dominated by the strong dependence on the VHS which produce peaks of the DOS for distinct fillings. If  $-V$  is larger than approximately a tenth of  $U$ , the Landau parameter  $F_0^s$  attains negative values in the full range of densities. If  $|V|$  is increased further,  $F_0^s$  becomes less than  $-1$ , primarily close to the densities where the VHS dominate, and a charge instability emerges.

However, for intermediate to large values of  $U/t$  and  $U/|V|$ , the charge instability is suppressed close to half filling. In fact, for increasing electronic correlations, we observe the formation of a pronounced peak of  $F_0^s$  around half filling. This rounded peak with positive values is the very signature of strong correlations and is entirely absent for weak coupling ( $U/t \simeq 1$ ). The tendency towards charge instability for negative  $V$  is quenched by electronic correlations in this regime—below half filling it may reemerge.

Finally, we would like to point to the observation that the effective interaction  $F_0^s$  may still be sizable for low densities, both for dominating repulsive  $U$  or for attractive  $V$ . This is a hallmark of 2D electronic systems, as in contrast  $F_0^s$  vanishes in the low density limit for generic 3D lattices, such as the cubic one [12]. This is found both in our formalism and in perturbation theory. In that respect, it is interesting to note that some 2D electronic systems have non-

negligible interaction effects even for low electron fillings which are not necessarily related to the presence of long-range Coulomb interactions. Specifically, the electron system at interfaces of  $\text{LaAlO}_3$  films on  $\text{SrTiO}_3$  substrates was interpreted as an electron liquid rather than an electron gas (see Ref. [8]). Moreover the metallic state, which is formed on  $\text{SrTiO}_3$  surfaces appears to support electronic correlations, unexpected for such a low density electron system (see Ref. [45]). Further analyses of these puzzling observations are required in this respect.

## Acknowledgements

This work was supported by the DFG through the TRR 80. R.F. is grateful to the Région Basse-Normandie and the Ministère de la Recherche for financial support. The authors acknowledge helpful discussions with V. H. Dao.

## 7. References

- [1] de Boer D, Haas C, and Sawatzky G A, Phys. Rev. B **29**, (1984), 4401.
- [2] van den Brink J, *The Hubbard Model with Orbital Degeneracy and in Polarizable Media*, Print Partners Ipskamp (1997).
- [3] Micnas R, Ranninger J, and Robaszkiewicz S, Rev. Mod. Phys. B **62** (1990), 113.
- [4] Sawatzky G A, Elfmov I S, Van Den Brink J, and Zaanen J, Europhys. Lett. **86** (2009), 17006; Berciu M, Elfmov I, and Sawatzky G A, Phys. Rev. B **79** (2009), 214507.
- [5] Ohtomo A and Hwang H Y, Nature **427** (2004) 423.
- [6] Thiel S, Hammerl G, Schmehl A, Schneider C W, and Mannhart J, Science **313** (2006), 1942.
- [7] Sing M, Berner G, Goß K, Müller A, Ruff A, Wetscherek A, Thiel S, Mannhart J, Pauli S A, Schneider C W, Willmott P R, Gorgoi M, Schäfers F, and Claessen R Phys. Rev. Lett. **102** (2009), 176805.
- [8] Breitschaft M, Tinkl V, Pavlenko N, Paetel S, Richter C, Kirtley J R, Liao Y C, Hammerl G, Eyert V, Kopp T, and Mannhart J, Phys. Rev. B **81** (2010) 153414.
- [9] Tinkl V, Breitschaft M, Richter C, and Mannhart J, Phys. Rev. B **86** (2012), 075116.
- [10] Hubbard J, Proc. R. Soc. London A **276** (1963), 238.
- [11] Vollhardt D, Rev. Mod. Phys. **56** (1984), 99.
- [12] Lhoutellier G, Frésard R, and Oleś A M, Phys. Rev. B **91** (2015), 224410.
- [13] Li T C, Wölfe P, and Hirschfeld P J, Phys. Rev. B **40** (1989), 6817.
- [14] Frésard R and Wölfe P, Int. J. of Mod. Phys. B **6** (1992), 685; *ibid.* **6** (1992), 3087.
- [15] Kotliar G and Ruckenstein A E, Phys. Rev. Lett. **57** (1986), 1362.
- [16] Pavlenko N and Kopp T, Phys. Rev. Lett. **97** (2006), 187001.
- [17] Brinkman W F and Rice T M, Phys. Rev. B **2** (1970), 4302.
- [18] Lilly L, Muramatsu A, and Hanke W, Phys. Rev. Lett. **65** (1990), 1379.
- [19] Yang I, Lange E, and Kotliar G, Phys. Rev. B **61** (2000), 2521.
- [20] Möller B, Doll K, and Frésard R, J. Phys.: Condens. Matter **5** (1993), 4847.
- [21] Frésard R, Dzierzawa M, and Wölfe P, Europhys. Lett. **15** (1991), 325.
- [22] Arrigoni E and Strinati G C, Phys. Rev. B **44** (1991), 7455.
- [23] Frésard R and Wölfe P, J. Phys.: Condens. Matter **4** (1992), 3625.
- [24] Igoshev P A, Timirgazin M A, Arzhnikov A K, and Irkhin V Y, JETP Lett. **98** (2013), 150.
- [25] Seibold G, Sigmund E, and Hizhnyakov V, Phys. Rev. B **57** (1998), 6937.
- [26] Seibold G and Lorenzana J, Phys. Rev. B **73** (2006), 144515.
- [27] Raczkowski M, Frésard R, and Oleś A M, Phys. Rev. B **73** (2006), 174525; Raczkowski M, Capello M, Poilblanc D, Frésard R, and Oleś A M, *ibid.* **76** (2007), 140505(R).
- [28] Raczkowski M, Frésard R, and Oleś A M, Europhys. Lett. **76** (2006), 128.
- [29] Zimmermann W, Frésard R, and Wölfe P, Phys. Rev. B **56** (1997), 10097.
- [30] Frésard R and Doll K, Proceedings of the NATO ARW *The Hubbard Model: Its Physics and Mathematical Physics*, eds. D. Baeriswyl, D. K. Campbell, J. M. P. Carmelo, F. Guinea, and E. Louis, San Sebastian (1993) (Plenum Press, 1995), p. 385.
- [31] Anderson P W, Science **235** (1987), 1196.
- [32] Frésard R, Kroha J, and Wölfe P, *Theoretical Methods for Strongly Correlated Systems*, edited by A. Avella and F. Mancini, Springer Series in Solid-State Sciences **171** (Springer-Verlag, Berlin Heidelberg, 2012) pp. 65-101.
- [33] Frésard R and Kopp T, Nucl. Phys. B **594** (2001), 769.
- [34] Frésard R, Ouerdane H, and Kopp T, Nucl. Phys. B **785** (2007), 286.
- [35] Jolicœur Th and Le Guillou J C, Phys. Rev. B **44** (1991), 2403.

- [36] Bang Y, Castellani C, Grilli M, Kotliar G, Raimondi R, and Wang Z, *Int. J. of Mod. Phys. B* **6** (1992), 531; Proceedings of the Adriatico Research Conference and Miniworkshop *Strongly Correlated Electrons Systems III*, eds. Yu Lu, G. Baskaran, A. E. Ruckenstein, E. Tossati (World Scientific Publishing Co., Singapore, 1992).
- [37] Metzner W and Vollhardt D, *Phys. Rev. Lett.* **62** (1989), 324; *Phys. Rev. B* **37** (1988), 7382; Metzner W, *Z. Phys. B* **77** (1989), 253.
- [38] Müller-Hartmann E, *Z. Phys. B* **74** (1989), 507.
- [39] Frésard R and Kopp T, *Ann. Phys. (Berlin)* **524** (2012), 175.
- [40] Frésard R and Lamboley M, *J. Low Temp. Phys.* **126** (2002), 1091.
- [41] Lavagna M, *Phys. Rev. B* **41** (1990), 142; *Helvetica Phys. Acta* **63** (1990), 310; *Int. J. Mod. Phys. B* **5** (1991), 885.
- [42] Vollhardt D, Wölffe P, and Anderson P W, *Phys. Rev. B* **35** (1987), 6703.
- [43] Li T C, Sun Y S and Wölffe P, *Z. Phys. B* **82** (1991), 369.
- [44] Li T C and Bénard P, *Phys. Rev. B* **50** (1994), 17837.
- [45] Meevasana W, King P D C, He R H, Mo S K, Hashimoto M, Tamai A, Songsiriritthigul P, Baumberger F, and Shen Z X, *Nat. Mater.* **10** (2011), 114.